

Persistent infrared spectral hole burning of Tb^{3+} in the glasslike mixed crystal $Ba_{1-x-y}La_xTb_yF_{2+x+y}$

S. P. Love,* C. E. Mungan, and A. J. Sievers

Laboratory of Atomic and Solid State Physics and Materials Science Center, Cornell University,
Ithaca, New York 14853-2501

J. A. Campbell

Department of Physics, University of Canterbury, Christchurch, New Zealand

Received October 14, 1991

Persistent IR spectral holes that exhibit glasslike characteristics—highly nonexponential low-temperature relaxation behavior and a broad distribution of barrier heights observable in thermal-cycling studies—have been produced in the inhomogeneously broadened $4.5\text{-}\mu\text{m } ^7F_6 \rightarrow ^7F_5$ electronic absorption band of the Tb^{3+} ion in the mixed crystal $Ba_{1-x-y}La_xTb_yF_{2+x+y}$. Investigations of six compositions, ranging from $x = 0, y = 0.005$ to $x = 0.30, y = 0.05$, reveal no hole burning for the $x = 0, y = 0.005$ case and a hole-burning quantum efficiency of the order of 5×10^{-7} with a weak dependence of the lanthanide fraction for $x + y \geq 0.05$. For all compositions with $x + y \geq 0.05$ hole behavior is virtually identical, with both the widths and the peak positions of the distributions of relaxation rates and barrier heights for these mixed crystals being typical of those found for glasses.

INTRODUCTION

Persistent nonphotochemical spectral hole burning, in which the defect electronic configuration is not changed by the hole-burning process, has been observed for a wide variety of impurities in glasses for both electronic^{1,2} and vibrational³⁻⁷ transitions of the impurity. In the standard model for nonphotochemical hole burning in glasses⁸ it is assumed that excitation of the impurity leads to a configuration change in the host surrounding the impurity, resulting in a shift of the impurity transition frequency away from the frequency of the exciting laser. The large number of nearly degenerate configurations available to the atoms of glasses, which is prerequisite for hole burning by this mechanism, is also invoked in the tunneling model^{9,10} for the low-temperature thermal properties of glasses. The observation¹¹ of glasslike low-temperature specific heat, thermal conductivity, and internal friction in the mixed crystal $Ba_{1-x}La_xF_{2+x}$ suggests that this class of material, like glasses, should have the multiple configurations necessary for nonphotochemical hole burning.

Here we report the production of persistent IR spectral holes (PIRSH's) in the inhomogeneously broadened $4.5\text{-}\mu\text{m } ^7F_6 \rightarrow ^7F_5$ electronic absorption band of the Tb^{3+} ion in the mixed crystal $Ba_{1-x-y}La_xTb_yF_{2+x+y}$. These PIRSH's display the characteristic properties of spectral holes burned in true glasses, including highly nonexponential hole relaxation on time scales ranging from a few minutes to many hours and a broad distribution of barriers observable in thermal-cycling studies.

EXPERIMENTAL DETAILS

All the $Ba_{1-x-y}La_xTb_yF_{2+x+y}$ crystals used in this study were grown by the Bridgeman method in graphite cru-

cibles under an Ar atmosphere by using an rf heated furnace. For hole-burning studies the samples, cut to a thickness of 1.0 cm, are mounted in an optical-access superfluid He immersion cryostat equipped with ZnSe inner windows and BaF_2 outer windows. The sample temperature is determined by using a calibrated C resistor attached to the sample. PIRSH burning is performed by using a tunable Pb-salt diode laser, operating in the 2220-cm^{-1} region, focused to a cw intensity at the sample typically of the order of 200 mW/cm^2 . PIRSH's are burned by holding the laser frequency constant for several minutes, then are probed with the same laser by sweeping the laser frequency through a region centered on the burn frequency. The width of any PIRSH produced is determined by using a calibrated Ge étalon, and the absolute frequency is determined with a grating monochromator, which also serves to select a single laser mode from the typically multimode diode output.

RESULTS AND DISCUSSION

General

In this investigation the inhomogeneously broadened IR absorption band necessary for PIRSH-burning experiments is provided by the Tb^{3+} ion. Like La, Tb forms a 3^+ ion when introduced into BaF_2 , and substitution of either La^{3+} or Tb^{3+} for Ba^{2+} results in an interstitial F^- ion that is necessary for charge neutrality.^{11,12} Similar glasslike behavior is therefore expected to be produced by the introduction of either La^{3+} or Tb^{3+} ions.

IR absorption spectra at 1.6 K for samples with various La and Tb concentrations are shown in Fig. 1. The overall effect of increasing the lanthanide concentration is to increase the degree of inhomogeneous broadening of the Tb^{3+} transitions, so that the sharp lines associated with

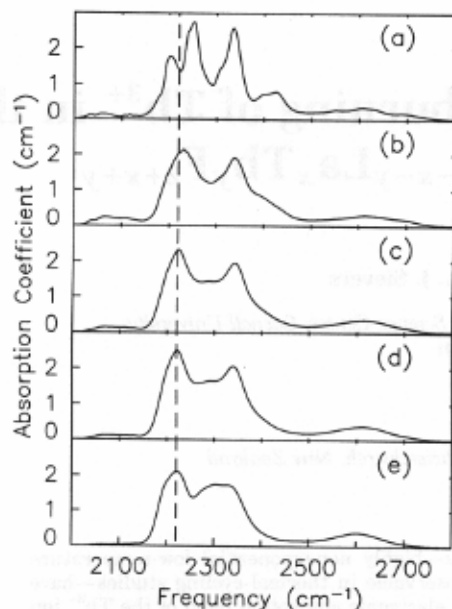


Fig. 1. IR absorption spectra of $\text{Ba}_{1-x-y}\text{La}_x\text{Tb}_y\text{F}_{2+x+y}$ mixed crystals at 1.6 K, showing the Tb^{3+} electronic absorptions. The La and Tb fractions, x and y , are (a) $x = 0, y = 0.05$; (b) $x = 0.05, y = 0.05$; (c) $x = 0.10, y = 0.05$; (d) $x = 0.15, y = 0.05$; and (e) $x = 0.3, y = 0.05$. The vertical dashed line indicates the laser frequency, 2220.2 cm^{-1} , used in determining the hole-burning quantum efficiency for each composition.

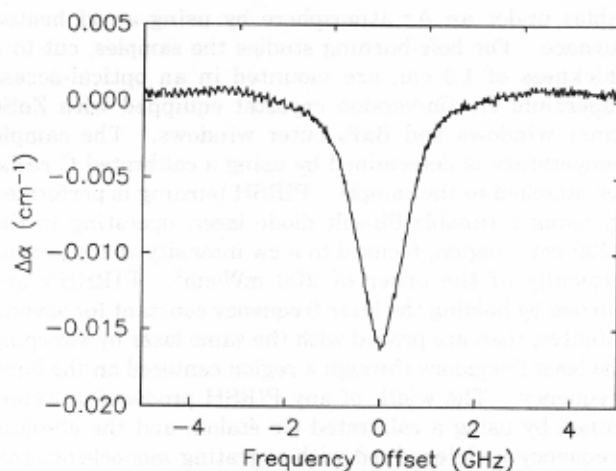


Fig. 2. Shown here is a persistent spectral hole produced in $\text{Ba}_{0.9}\text{La}_{0.05}\text{Tb}_{0.05}\text{F}_{2.1}$ at 1.6 K by a 15-min burn at 2198 cm^{-1} at an intensity of 300 mW/cm^2 . Plotted is the laser-induced change in the absorption coefficient, $\Delta\alpha$, as a function of the offset from the burning frequency.

specific defect clusters that are apparent at relatively low concentrations eventually broaden and merge into a single inhomogeneous band at the highest concentrations.

PIRSH burning has been observed for samples of $\text{Ba}_{1-x-y}\text{La}_x\text{Tb}_y\text{F}_{2+x+y}$ with the following nominal (melt) compositions: $y = 0.05$; $x = 0, 0.05, 0.10, 0.15, 0.3$. Figure 2 shows the PIRSH produced at 1.6 K in the $x = y = 0.05$ sample by a 15-min burn at 2198 cm^{-1} at an intensity of 300 mW/cm^2 .

A possible mechanism for spectral hole burning, which we rule out here, would be an internal relaxation bottleneck in the Tb^{3+} ion itself. We do observe hole burning by such an internal optical-pumping mechanism in another rare-earth-doped alkaline-earth halide system,

$\text{CaF}_2:\text{Pr}^{3+}$. In that system we observe spectral hole burning for transitions in the crystal field split ${}^3H_4 \rightarrow {}^3H_5$ manifold at $\sim 4.5 \mu\text{m}$. Preliminary results show that for CaF_2 with 1.0 at. % Pr^{3+} the transition at 2194 cm^{-1} produces holes $\sim 140 \text{ MHz}$ wide (FWHM) at 1.6 K with simple antihole wings spread over a few hundred megahertz, whereas the 2182-cm^{-1} transition displays a complicated series of holes and antiholes, with an antihole falling, surprisingly, at the laser frequency. All holes observed in the ${}^3H_4 \rightarrow {}^3H_5$ manifold relax exponentially at 1.6 K with a lifetime of $36 \pm 1 \text{ s}$. This behavior is reminiscent of that observed for Pr^{3+} hole burning in the visible region, for which the hole-burning mechanism is optically pumped population redistribution among the hyperfine^{13,14} or superhyperfine¹⁵⁻¹⁷ split ground-state levels of the Pr^{3+} ion, with hole filling occurring at the characteristic spin-lattice relaxation rate.¹⁸ The present results for the $\text{CaF}_2:\text{Pr}^{3+} {}^3H_4 \rightarrow {}^3H_5$ transitions are, to our knowledge, the first instances of hole burning by this optical-pumping mechanism to be observed in the mid-IR region.

In order to test whether PIRSH burning in the $\text{Ba}_{1-x-y}\text{La}_x\text{Tb}_y\text{F}_{2+x+y}$ system could be due to such a mechanism, we prepared a sample with no La and only 0.5% Tb. Since hole burning by means of internal population redistribution of the ion itself should occur at any concentration, this low-concentration sample would display PIRSH burning similar to that for the other samples if this optical-pumping mechanism were responsible. Attempts to observe PIRSH burning in this $x = 0$ and $y = 0.005$ sample, however, yielded null results, thus ruling out the internal optical-pumping mechanism for the $\text{Ba}_{1-x-y}\text{La}_x\text{Tb}_y\text{F}_{2+x+y}$ system. That the hole-burning mechanism in $\text{Ba}_{1-x-y}\text{La}_x\text{Tb}_y\text{F}_{2+x+y}$ is not internal optical pumping is further emphasized by the highly nonexponential nature of the hole decay, with very long hole lifetimes (many hours) occurring at the slow end of the distribution of relaxation rates.

Quantum Efficiencies

To investigate to what extent the La^{3+} concentration affects the hole-burning quantum efficiency, we have measured the hole growth as a function of time for all five compositions under identical conditions (1.6 K, laser frequency 2220.2 cm^{-1} , and intensity 160 mW/cm^2), using the same diode-laser mode for all samples. We then calculate the hole-burning quantum efficiency, η , from the short-time hole growth behavior by using the definition of Moerner *et al.*,¹⁹ where η can be expressed in terms of experimentally accessible quantities as

$$\eta = \frac{[dT(t)/dt]_{t=0}}{4(I/h\omega_L)(1/\pi\gamma_{\text{hole}})(S_{\text{tot}}/N_{\text{tot}})T_0(1 - T_0 - R)}, \quad (1)$$

where $T(t)$ is the time-dependent external sample transmittance at the laser frequency ω_L , T_0 is the initial external transmittance, R is the reflectance, I is the external laser intensity at the sample, and γ_{hole} is the hole width (FWHM) measured in the small-hole limit (equal to twice the homogeneous width), expressed in inverse centimeters. S_{tot} is the integrated absorption strength of the inhomogeneous band being burned; i.e., $S_{\text{tot}} = \int \alpha(\omega)d\omega$, with the integral performed over the inhomogeneous band. N_{tot} is the density of centers (per cubic centimeter)

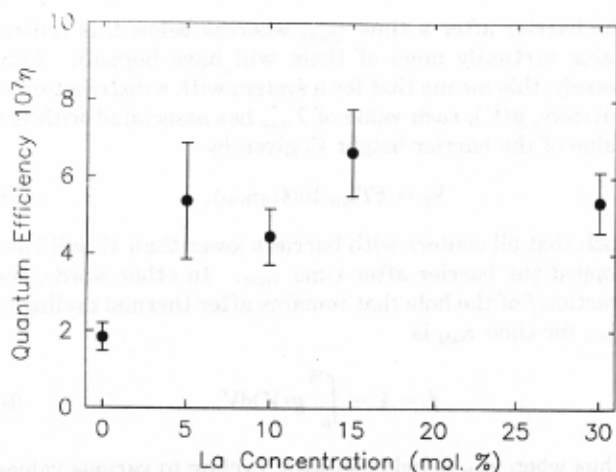


Fig. 3. Hole-burning quantum efficiencies at 1.6 K for five $\text{Ba}_{1-x-y}\text{La}_x\text{Tb}_y\text{F}_{2+x+y}$ compositions, all with Tb fraction $y = 0.05$, plotted as a function of the La fraction, x . Identical burning conditions and an intensity of 160 mW/cm^2 at 2220.2 cm^{-1} were used for all compositions.

giving rise to the inhomogeneous absorption band. Here we use the nominal 5% Tb concentration, so that $N_{\text{tot}} = 8.4 \times 10^{20} \text{ cm}^{-3}$, and we define the inhomogeneous band as being the entire $\text{Tb}^{3+} {}^7F_6 \rightarrow {}^7F_5$ region, from approximately 1800 to 3000 cm^{-1} , so that $S_{\text{tot}} = 460 \pm 20 \text{ cm}^{-2}$. For all compositions the hole width (FWHM) in the small-hole limit at this frequency is $0.84 \pm 0.04 \text{ GHz}$.

The measured quantum efficiency is plotted as a function of La^{3+} concentration in Fig. 3. After an initial increase in η from approximately 2×10^{-7} for the 0% La sample to approximately 5.5×10^{-7} for the 5% La case, the quantum efficiency remains constant, to within experimental error, between approximately 5×10^{-7} and 6×10^{-7} . We note that these values fall well within the typical range for PIRSH-burning systems; the low absorption cross section for the ${}^7F_6 \rightarrow {}^7F_5$ transition, however, makes this system relatively difficult for hole burning.

One might have expected a more dramatic increase in the quantum efficiency with increasing La^{3+} concentration on the grounds that increased La^{3+} concentration would increase the fraction of Tb^{3+} sites having sufficient local configurational multiplicity for hole burning. The results, however, suggest that such an effect is already nearly saturated by the presence of Tb^{3+} itself at concentrations of 5%. This inference is in agreement with the idea that the multiple configurations associated with hole burning are somehow associated with the F^- interstitials, which are produced by the introduction of any trivalent lanthanide, either La^{3+} or Tb^{3+} . The absence of hole burning for the low-concentration 0.5% Tb sample with no La confirms that hole burning occurs only when the trivalent impurity concentration, and hence the density of F^- interstitials, is greater than some critical value, somewhere between 0.5% and 5%.

Low-Temperature Hole Relaxation

Monitoring the evolution of the hole size after burning ceases reveals highly nonexponential refilling of the PIRSH's in $\text{Ba}_{1-x-y}\text{La}_x\text{Tb}_y\text{F}_{2+x+y}$ following a form virtually identical to that observed for PIRSH's burned in glasses. Figure 4 shows the integrated area of the PIRSH burned and probed at 1.6 K proportional to the number of centers

remaining in the hole-burned configuration, plotted as a function of time after the burning laser is removed, for two compositions, ($x = y = 0.05$) and ($x = 0.30, y = 0.05$). The PIRSH relaxation behavior for the two compositions is identical within experimental error.

As is the case with glasses,^{3-7,20,21} the 1.6-K hole-relaxation behavior is well described by a simple model in which it is assumed that relaxation proceeds by tunneling between the ground-state configurations. The rate at which a given center relaxes from the burned to the unburned configuration is given by

$$\Gamma_{\text{BU}} = \Gamma_0 \exp(-\lambda), \quad (2)$$

where Γ_0 is an attempt frequency, assumed to be of the order of a phonon frequency, and λ is the tunneling parameter, of the general form $(2mV)^{1/2}d/h$, where m is the mass of the tunneling entity, V the barrier height, and d the width of the barrier. In order to take into account the distribution of environments seen by the defect, we simply allow the tunneling parameter λ to assume a Gaussian distribution about some center value λ_0 , as suggested by Jankowiak et al.^{20,21}:

$$G(\lambda) = (1/\pi^{1/2}\sigma) \exp[-(\lambda - \lambda_0)^2/\sigma^2]. \quad (3)$$

Thus, if $N_B(0)$ is the total number of centers initially in the hole-burned state, the number of centers having burned-to-unburned relaxation rates between $\Gamma_0 \exp(-\lambda)$ and $\Gamma_0 \exp[-(\lambda + d\lambda)]$ is $N_B(0)G(\lambda)d\lambda$. The number of centers with this relaxation rate remaining after time t is then given by

$$dN_{B,\lambda}(t) = N_B(0)G(\lambda)d\lambda \exp[-\Gamma_0 t \exp(-\lambda)], \quad (4)$$

and so the total number of centers remaining in the hole-burned configuration after time t is obtained by integrating Eq. (4) over all λ :

$$\frac{N_B(t)}{N_B(0)} = \frac{1}{\pi^{1/2}\sigma} \int_0^\infty \exp[-(\lambda - \lambda_0)^2/\sigma^2] \exp[-\Gamma_0 t \exp(-\lambda)] d\lambda. \quad (5)$$

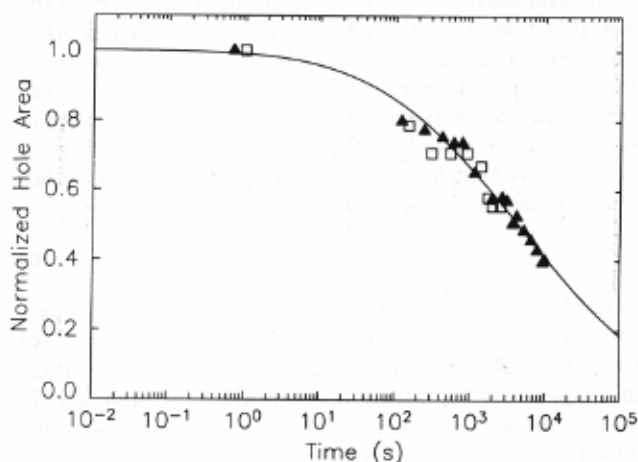


Fig. 4. PIRSH relaxation at 1.6 K for two compositions in the $\text{Ba}_{1-x-y}\text{La}_x\text{Tb}_y\text{F}_{2+x+y}$ system, $x = 0.05, y = 0.05$ (filled triangles) and $x = 0.05, y = 0.3$ (open squares). Plotted for each case is the integrated area of the spectral hole as a function of time after burning ceases, with the hole area normalized to unity at $t = 0$. The initial holes were burned for 15 min at 2220 cm^{-1} . The solid curve is a fit to a Gaussian distribution of tunneling parameters (see text).

A fit of the data using Eq. (5) for both compositions is shown by the solid curve in Fig. 4, where the fit parameters are the Gaussian distribution width, $\sigma = 4.61$, and the dominant relaxation rate $\Gamma_0 \exp(-\lambda_0) = 1.28 \times 10^{-4} \text{ s}^{-1}$. These values, both the distribution width and the dominant relaxation rate, are typical of those observed for glasses. For instance, various experiments on the 1.6-K relaxation of holes in the SeH vibrational band in glassy Se could be fitted by using Eq. (5) with parameter values ranging from $\sigma = 2.07$ and $\Gamma_0 \exp(-\lambda_0) = 5.5 \times 10^{-4} \text{ s}^{-1}$ to $\sigma = 2.70$ and $\Gamma_0 \exp(-\lambda_0) = 1.1 \times 10^{-3} \text{ s}^{-1}$, depending on the burning laser intensity used, whereas for holes in the SH vibrational band in glassy As_2S_3 the parameters ranged from $\sigma = 4.93$ and $\Gamma_0 \exp(-\lambda_0) = 3.6 \times 10^{-3} \text{ s}^{-1}$ to $\sigma = 6.56$ and $\Gamma_0 \exp(-\lambda_0) = 1.7 \times 10^{-1} \text{ s}^{-1}$.³⁻⁷

The important aspect of these results is that they show that hole burning in this system is not the result of just one or just a few types of configurational change, such as a single F^- interstitial undergoing a particular kind of site-to-site hopping, for example, but is the result of a huge family of configurational changes for which there is a continuous distribution of barrier sizes. This is one of the essential hallmarks of glassy behavior.

Distribution of Barrier Heights: Thermal-Cycling Experiments

While low-temperature PIRSH-relaxation experiments permit the determination of a distribution of tunneling parameters for the centers involved in hole burning, the quantities that go into the tunneling parameter, the height and the width of the barriers, and the mass of the tunneling entity cannot be disentangled by this kind of experiment.

The distribution of barrier heights for this system, however, can be determined separately through a thermal-cycling experiment of the sort recently demonstrated by Köhler *et al.*²² In this experiment a hole is burned and measured at 1.6 K; the sample is quickly heated to some maximum temperature T_{max} , held at that temperature for a fixed time τ_{hold} , and then quickly cooled to 1.6 K; and the hole is remeasured. The fraction of the hole that remains after this thermal cycle (corrected for the fraction that would have been lost anyway through low-temperature tunneling) is a measure of the fraction of centers whose barriers to hole refilling are greater than some critical height, V_0 , determined by T_{max} and τ_{hold} . To see this relationship, note that for a single barrier height V the Arrhenius thermal barrier hopping rate R is

$$R = \Omega_0 \exp(-V/kT), \quad (6)$$

where k is Boltzmann's constant and Ω_0 is an attempt frequency of the order of a phonon frequency, so that if we instantaneously raise the temperature to T_{max} , maintain the temperature for a time τ_{hold} , and then instantaneously cool the sample, the fraction f of centers that will not have hopped the barrier after time τ_{hold} is

$$f = \exp[-\Omega_0 \tau_{\text{hold}} \exp(-V/kT_{\text{max}})]. \quad (7)$$

The key to this argument is that, for fixed Ω_0 , V , and τ_{hold} , this function can be approximated quite well as a unit-step function in T_{max} : Above some critical value of T_{max} virtually all centers with barrier height V will have hopped

the barrier after a time τ_{hold} , whereas below this critical value virtually none of them will have hopped. Conversely, this means that for a system with a distribution of barriers, $g(V)$, each value of T_{max} has associated with it a value of the barrier height V_0 given by

$$V_0 = kT_{\text{max}} \ln(\Omega_0 \tau_{\text{hold}}), \quad (8)$$

such that all centers with barriers lower than V_0 will have hopped the barrier after time τ_{hold} . In other words, the fraction f of the hole that remains after thermal cycling to T_{max} for time τ_{hold} is

$$f = 1 - \int_0^{V_0} g(V) dV. \quad (9)$$

Thus when τ_{hold} is held constant, cycling to various values of T_{max} allows one to map out the distribution $g(V)$. If one plots the fraction remaining, f , versus V_0 obtained from T_{max} by means of Eq. (8), the distribution $g(V)$ is obtained by taking the derivative of f with respect to V_0 .

Figure 5 shows the results of a thermal-cycling experiment for the $\text{Ba}_{0.9}\text{La}_{0.05}\text{Tb}_{0.05}\text{F}_{2.1}$ sample. For each data point in Fig. 5 a hole was burned at 1.6 K for 5 min at 2198 cm^{-1} at an intensity of 300 mW/cm^2 . After a hole measurement was obtained at 1.6 K, the sample was warmed as quickly as possible to the maximum temperature T_{max} , maintained at that temperature for a time τ_{hold} of 30 s, then immediately cooled to 1.6 K, at which time the hole was remeasured. To obtain the data points plotted in Fig. 5, the final hole size was divided by its size before thermal cycling, then corrected for the finite time required for warming and cooling. This correction is necessary because the entire cycle for a single data point typically takes approximately 5–7 min, during which time a hole maintained at 1.6 K would have decayed to ~75% of

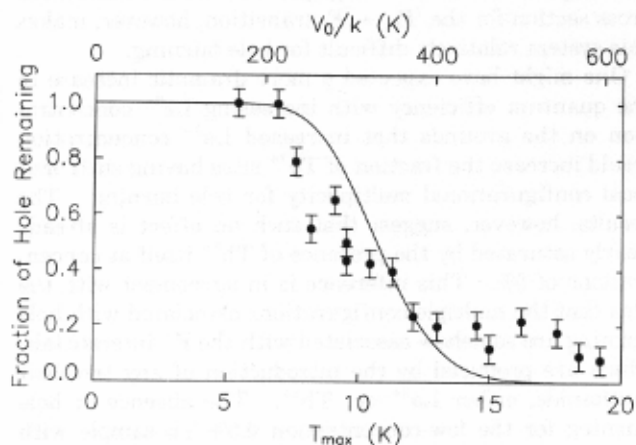


Fig. 5. Thermal PIRSH erasure results for $\text{Ba}_{0.9}\text{La}_{0.05}\text{Tb}_{0.05}\text{F}_{2.1}$. Each data point was obtained by burning a hole at 1.6 K for 5 min with 300-mW/cm^2 intensity at 2198 cm^{-1} ; warming the sample to the maximum temperature T_{max} (bottom scale), holding it at T_{max} for 30 s, and then cooling it; and remeasuring the hole at 1.6 K. Plotted is the fraction of the hole remaining, corrected for the natural 1.6-K relaxation that would have occurred during the time taken by the experiment. The top scale indicates the barrier heights, V_0 , corresponding to each T_{max} , for an assumed attempt frequency of 10^{12} s^{-1} . The fraction of the hole remaining then corresponds to the fraction of centers having a barrier height $>V_0$. The solid curve indicates a fit to these data based on the Gaussian distribution of tunneling parameters obtained from Fig. 4 (see text).

its initial size (compare Fig. 4). To take this decay into account, we multiply the ratio of the final to the initial hole size by a factor obtained from the fit of Eq. (5) to the 1.6-K relaxation shown in Fig. 4. It is these final values that are plotted in Fig. 5 as a function of T_{\max} .

Examination of Fig. 5 reveals that the most rapid increase in barrier hopping with increasing T_{\max} , corresponding to the main peak of the distribution of barrier heights, occurs at approximately $T_{\max} = 9$ K. By using Eq. (8) with our τ_{hold} of 30 s and assuming an attempt frequency $\Omega_0 = 10^{12} \text{ s}^{-1}$, we find that this temperature corresponds to a peak in the distribution $g(V)$ near $V/k = 280$ K. The nearly flat region from approximately $T_{\max} = 13$ K to $T_{\max} = 17$ K [or from $V/k = 400$ K to $V/k = 530$ K, according to Eq. (8)] corresponds to a region in which $g(V)$ is nearly zero. The final decrease in the hole fraction above $T_{\max} = 17$ K appears to indicate a second smaller peak in $g(V)$ somewhere near $T_{\max} = 19$ K or $V/k = 590$ K, though here the experimental uncertainty is quite large.

If we now use these results for the distribution of barrier height $g(V)$ together with the distribution of tunneling parameters $G(\lambda)$ obtained from the 1.6-K hole relaxation, we can obtain some idea of the mass of the tunneling entity and the tunneling distance. Starting with the Gaussian $G(\lambda)$ used to fit the data of Fig. 4, we use the square barrier form of the tunneling parameter,

$$\lambda^2 = 2mVd^2/\hbar^2, \quad (10)$$

to transform $G(\lambda)$ into $g(V)$ and fit this $g(V)$ to the results of Fig. 5, by means of Eq. (9), using the product md^2 as an adjustable parameter. The solid curve in Fig. 5 shows the resulting fit. For this fit we set both the tunneling attempt frequency [Eq. (2)] and the Arrhenius attempt frequency [Eq. (6)] equal to 10^{12} s^{-1} and used the experimental value of $\tau_{\text{hold}} = 30$ s. The value of md^2 used to obtain this fit is $1.67 \times 10^{-45} \text{ kg m}^2$ or, equivalently, $\sim 100 \text{ amu } \text{\AA}^2$. Given that the F mass is 19 amu, while the remaining species' masses range from 137.3 amu for Ba to 158.9 amu for Tb, this value appears to be physically reasonable; the tunneling involved in the 1.6-K relaxation could, for instance, involve several F^- interstitials moving $\sim 1 \text{ \AA}$. We emphasize, however, that, since many types of configuration are probably involved in the hole burning, md^2 , like V , should take on a broad distribution of values, and this analysis should be viewed mainly as a verification that the assumption that relaxation occurs by tunneling at 1.6 K is physically reasonable.

SUMMARY AND CONCLUSIONS

In summary, in the $\text{Ba}_{1-x-y}\text{La}_x\text{Tb}_y\text{F}_{2+x+y}$ system we have observed persistent spectral hole burning that displays striking similarities to nonphotochemical hole burning in glasses. Both the highly nonexponential hole relaxation at 1.6 K and the broad distribution of barrier heights seen in thermal hole-erasure measurements are typical of glassy systems. Taken together, moreover, the two types of experiment support the tunneling interpretation of the low-temperature hole relaxation. Over the composition range 5–35% combined La and Tb concentration, the hole-burning quantum efficiency was found to be only

weakly dependent on the lanthanide concentration, though no hole burning was observed for the 0.5% Tb material. Thus future studies intended to elucidate the role of lanthanide doping in producing the glasslike multiple configurations necessary for hole burning should concentrate on materials with lanthanide fractions of less than 5%.

ACKNOWLEDGMENTS

We thank D. G. Cahill and R. O. Pohl for valuable discussions and E. Havelaar for assistance in growing several of the crystals used in this study. Research at Cornell was supported by the National Science Foundation, grant DMR-87-14600, and by the U.S. Army Research Office, grant DAAL03-89-K0053.

*Present address, Isotope and Structural Chemistry Group (INC-4), Los Alamos National Laboratory, Los Alamos, New Mexico 87545.

REFERENCES

1. J. M. Hayes, R. Jankowiak, and G. J. Small in *Persistent Spectral Hole Burning: Science and Applications*, W. E. Moerner, ed. (Springer-Verlag, Berlin, 1988), Chap. 5.
2. R. M. Macfarlane and R. M. Shelby, in *Persistent Spectral Hole Burning: Science and Applications*, W. E. Moerner, ed. (Springer-Verlag, Berlin, 1988), Chap. 4.
3. S. P. Love and A. J. Sievers, "Persistent infrared spectral hole burning of the sulfur-hydrogen stretch mode in hydrogenated As_2S_3 glass," *Chem. Phys. Lett.* **153**, 379 (1988).
4. S. P. Love and A. J. Sievers, "Persistent IR spectral hole burning in chalcogenide glasses," *J. Lumin.* **45**, 58 (1990).
5. S. P. Love and A. J. Sievers, in *Advances in Disordered Semiconductors, Volume III—Transport, Correlation, and Structural Defects*, H. Fritzsche, ed. (World Scientific, Singapore, 1990), pp. 27–61.
6. S. P. Love, A. J. Sievers, B. L. Halfpap, and S. M. Lindsay, "Effects of network topology on low-temperature relaxation in Ge-As-Se glasses, as probed by persistent infrared spectral hole burning," *Phys. Rev. Lett.* **65**, 1792 (1990).
7. S. P. Love, "Persistent infrared spectral hole burning studies of chalcogenide glasses and other disordered semiconductors," Ph.D. dissertation (Cornell University, Ithaca, NY, 1991).
8. J. M. Hayes and G. J. Small, "Non-photochemical hole burning and impurity site relaxation processes in organic glasses," *Chem. Phys.* **27**, 151 (1978).
9. P. W. Anderson, B. I. Halperin, and C. M. Varma, "Anomalous low-temperature thermal properties of glasses and spin glasses," *Philos. Mag.* **25**, 1 (1971).
10. W. A. Phillips, "Tunneling states in amorphous solids," *J. Low Temp. Phys.* **7**, 351 (1972).
11. D. G. Cahill and R. O. Pohl, "Low-energy excitations in the mixed crystal $\text{Ba}_{1-x}\text{La}_x\text{F}_{2+x}$," *Phys. Rev. B* **39**, 10477 (1989).
12. C. R. A. Catlow, A. V. Chadwick, and J. Corish, "The defect structure of anion excess CaF_2 ," *J. Solid State Chem.* **48**, 65 (1983).
13. L. E. Erickson, "Optical measurement of the hyperfine splitting of the 1D_2 metastable state of Pr^{3+} in LaF_3 by enhanced and saturated absorption spectroscopy," *Phys. Rev. B* **16**, 4731 (1977).
14. L. E. Erickson, "Hyperfine interaction in the lowest levels of the 3H_4 and 1D_2 states of trivalent praseodymium in yttrium aluminum perovskite (YAlO_3)," *Phys. Rev. B* **19**, 4412 (1979).
15. R. M. Macfarlane, R. M. Shelby, and D. P. Burum, "Optical hole burning by superhyperfine interactions in $\text{CaF}_2:\text{Pr}^{3+}$," *Opt. Lett.* **6**, 593 (1981).
16. D. P. Burum, R. M. Shelby, and R. M. Macfarlane, "Hole burning and optically detected fluorine NMR in $\text{Pr}^{3+}:\text{CaF}_2$," *Phys. Rev. B* **25**, 3009 (1982).

